IOP Publishing Journal of Physics B: Atomic, Molecular and Optical Physics
J. Phys. B: At. Mol. Opt. Phys. **50** (2017) 115005 (9pp) https://doi.org/10.1088/1361-6455/aa6fc4

Overlapping photo-ionized doubly excited resonance series for Li^+ ion

T K Fang[1], X Gao[2] and T N Chang[3]

[1] Department of Physics, Fu Jen Catholic University, New Taipei City, Taiwan 24205, Republic of China
[2] Beijing Computational Science Research Center, Beijing, 100193, People's Republic of China
[3] Department of Physics, Univ. of Southern California, LA, CA 90089-0484, United States of America

E-mail: 051420@mail.fju.edu.tw

Received 21 December 2016, revised 9 April 2017
Accepted for publication 27 April 2017
Published 15 May 2017

Abstract

Based on two different approaches, the B-spline-based K-matrix method and the eigenchannel R-matrix method, we present a detailed theoretical study on the photoionization from the ground and bound excited $1s2s\ ^1S$ and $1s2p\ ^1P$ states of an Li^+ ion to continua between the $N = 2$ and $N = 3$ thresholds, dominated by overlapping doubly excited resonance series embedded in multiple singly ionized channels. The nearly identical theoretical spectra from these two different calculations, together with the excellent agreement between the length and velocity results, suggests that our study has successfully led to a reliable estimate of the Li^+ photoionization spectra. In addition to identifying all overlapping doubly excited autoionization series, our calculated spectrum is in good agreement with the only observed data for two broad resonances. Our study has also shown that the strong interaction between neighboring resonances from different resonance series, which is responsible for the level crossing for in the He atom, is substantially smaller due to a stronger nuclear attraction to atomic electrons for the two-electron ions.

Keywords: photoionization, autoionization, line shapes, level crossing

(Some figures may appear in colour only in the online journal)

1. Introduction

We have recently studied in detailed the interactions between multiple overlapping doubly excited resonance series of the ^1S and ^1D converging to the degenerate $3s$, $3p$, and $3d$ thresholds corresponding to the principle quantum number $N = 3$ for He atom based on the theoretical spectra for photoionization from the bound excited $1s2p\ ^1P$ state [1]. In particular, our investigation has shown the presence of a somewhat unexpected level crossing between two strongly interacting doubly excited resonances series, both for the ^1S and ^1D symmetries. These level crossings could be attributed to the fact that for a two-electron atomic system, the doubly excited resonance series above the first ionization threshold are difficult to classify in terms of the usual LS coupling, with a single pair of electronic configuration of two one-electron orbital angular quantum numbers $\ell_1\ell_2$, due to the presence of the degenerate higher ionization thresholds with $N > 1$ (i.e., $2s$ and $2p$ for $N = 2$ and $3s$, $3p$, and $3d$ for $N = 3$). Instead, they are classified by the KT coupling in terms of a set of correlated quantum numbers (K, T, and A) in the form of $(K, T)^A_n$ [2]. It would be interesting to find out if such level crossing is a general property as a result of the presence of the $N > 1$ degenerate thresholds of a two-electron system.

Experimentally, the photoionization of other two-electron system, beyond the neutral He atom, was investigated about a decade ago [3] for Li^+ ion from its ground state at photon energies up to 185 eV below the $N = 3$ ionization threshold, using the photon-ion merged-beam at APL (Advanced Light Source) following a few earlier observations [4, 5]. The observed ^1P spectra below the $N = 2$ ionization threshold were already well categorized by the theory. Above the $N = 2$ threshold, however, only two of the dominating ^1P resonances, $_3(1, 1)^+_3$ and $_3(1, 1)^+_4$ with KT classification, were resolved among the five expected ^1P resonances series. The observed energies and widths of these two relatively broad resonances are in good agreement with the existing theoretical results [6, 7]. All of the five

resonances series were identified theoretically in a detailed complex-rotation calculation [6], although no energy spectrum was available.

Similar to our recent study on He, we present in this paper the theoretical investigation of the overlapping ^1S and ^1D doubly excited resonance series embedded in multiple ionization channels of the photoionization spectra of Li^+ ions from the bound excited $1s2p\ ^1P$ state. We will first show the well-resolved three ^1S and six ^1D doubly excited resonance series between the $N = 2$ and $N = 3$ thresholds. In addition, we present in details the spectra for the five ^1P resonance series from the ground and the metastable $1s2s\ ^1S$ state, again, between the $N = 2$ and $N = 3$ ionization thresholds. In particular, we look for the level crossing, if any, similar to those we identified from the He photoionization spectra by examining the partial cross sections into all ionization channels and if it could be linked to the strong interaction between the neighboring resonance series.

Our theoretical spectra are derived from two distinctive theoretical approaches, the B-spline-based K-matrix method (BSK) [8, 9] and the eigenchannel R-matrix method (ECR) [10, 11], same as those applied in our recent study on He atom. The overall agreement is excellent between these two calculations over an extended energy region, which we will show in section 3. The agreement between the length and velocity results to better than 1% from both calculations further supports the quantitative reliability of our theoretical study. It is our hope that this study will offer the necessary impetus and the challenge to renew the experimental interest with the substantial improvement in energy resolution as well as the more intense light source over a greater spectral region during the past decade.

We will review briefly some of the key elements of the BSK and ECR approaches in section 2 and point out how to identify each of the doubly excited resonance through the energy variation of the sum of the eigenphase shifts over the contributing eigenchannels. In section 3, we will present the results and the discussion of our calculated energy spectra for the three ^1S, the five ^1P, and the six ^1D resonance series between the $N = 2$ and $N = 3$ ionization thresholds.

2. Theoretical approaches

As we pointed out earlier that two distinctive theoretical approaches, the BSK method [8, 9] and the ECR method [10, 11], are employed in the present study. For ionization into multiple ionization channels, both approaches rely on the use of eigenchannels, similar to the normal modes of a complex system, for the dynamics of the physical processes. We should reiterate that the *eigenchannels* are intimately related to the dynamics of the atomic process, but, they do not represent directly the individual atomic states. Although the detailed formulation and the computation procedures are very different from those two approaches, the resulting energy spectra as shown in section 3 are in excellent agreement with each other. In this section, we review only briefly the basics of the BSK and ECR approaches.

2.1. BSK method

Starting from an earlier B-spline-based configuration interaction method (BSCI) [8] for single ionization channel and similar to the usual K-matrix approaches [12, 13], a BSK method for the multi-channel photoionization was first proposed by Fang and Chang [9]. In essence, an eigenchannel Γ at a total energy E is expressed by a linear combination of all individual open channel wavefunctions $|\Phi_{\gamma_o E}\rangle$ with an eigenphase shift η_Γ and a transformation matrix $U_{\gamma_o\Gamma}(E)$, i.e. [9]

$$|\Gamma E\rangle = \sum_{\gamma_o} |\Phi_{\gamma_o E}\rangle\ U_{\gamma_o\Gamma}(E)\ \cos\eta_\Gamma(E), \tag{1}$$

where the eigenstate $|\Gamma E\rangle$ satisfies the *orthonormality* relation

$$\langle \Gamma' E'\ |\Gamma E\ \rangle = \delta_{\Gamma'\Gamma}\,\delta(E' - E). \tag{2}$$

The eigenphase shift η_Γ and the transformation matrix $U_{\gamma_o\Gamma}(E)$ are obtained by diagonalizing the *on the energy shell* K-matrix, i.e.,

$$\sum_\gamma \langle \gamma_o E\ |\ K(E)|\gamma E\ \rangle\, U_{\gamma\Gamma} = -\pi^{-1}\tan\eta_\Gamma\ U_{\gamma_o\Gamma}. \tag{3}$$

The K-matrix is expressed as a set of coupled integral equations given explicitly by equation (11) in [9]. The sum of η_Γ over all eigenchannels, i.e., $\eta_{\rm tot} = \sum\eta_\Gamma$, increases by a total of π as the energy increases across an isolated resonance. Following the well established procedure in atomic structure calculation, the width of a resonance can be derived from the energy variation of $\eta_{\rm tot}$ [14]. We should point out that all interactions between $|\Phi_{\gamma_o E}\rangle$ are included in $U_{\gamma_o\Gamma}(E)$ and η_Γ. The partial cross section for each open channel γ in unit of a_0^2 is given by

$$\sigma_\gamma = 4\pi^2\alpha\, f_{\gamma I}, \tag{4}$$

where the effective oscillator strengths $f_{\gamma I}$ from an initial state I, corresponding to length and velocity approximations are given explicitly by equations (22) and (23) in [9], respectively. The total photoionization cross section $\sigma_{\rm tot}$ is thus given by the sum of the partial cross sections over all open channels, i.e., $\sigma_{\rm tot} = \sum_\gamma \sigma_\gamma$.

2.2. ECR method

By separating the configuration space into subregions with a judicial choice of appropriate wave functions for the core and outer regions connected at their common boundary $r = r_o$, the R-matrix approach has managed successfully in treating many of the dynamic processes in atomic physics [15–18]. More recently, Gao and Li have extended the nonrelativistic and relativistic versions of the ECR approaches from the earlier versions of the Breit–Paul [16] and Dirac R-matrix [17] codes into what are referred to as the R-eigen [10] and R–R-eigen [11] codes, respectively. For the R-eigen code, the one-particle Hamiltonian is nonrelativistic with or without the Breit–Pauli terms, whereas the one-particle relativistic Dirac–Coulomb Hamiltonian is applied for the R–R-eigen code. The physical

parameters associated with the multichannel quantum defect theory (MQDT) are first calculated from the scattering matrices in ECR approach for both the discrete and continuous energy levels and the physical quantities of interest are then derived from the MQDT procedure [19–22].

At an energy E, only a finite number ($i \leqslant n_p$) of physically allowed ionized channels, known as the physical channels, contribute directly to the spectral structure. All other contributing channels ($j > n_p$) with higher core states energy are called the computational channels. The reaction matrix $K(E)$ is calculated with the standing-wave expressions for the eigenchannel wave function $\Psi_i(E)$ on the boundary of the reaction zone, i.e., at $r_o = r_{N+1}$

$$\Psi_i(E) = \Phi_i f_i(r_o, E) + \sum_{j=1}^{n_p} \Phi_j g_j(r_o, E) K_{ij} + \sum_{j=n_p+1} \Phi_j \Theta_j(r_o, E), \quad i \leqslant n_p, \tag{5}$$

where i and j are the channel indices. For the physical channel, the N-electron target-state core wave function Φ_i is combined with the angular and spin parts of the wave function of the $(N+1)$th electron in the ith channel and the corresponding regular and irregular Coulomb wave functions, $f_i(r, E)$ and $g_i(r, E)$, which are modified by the appropriate long-range polarization interactions that cover the entire set of one-electron orbitals, with both negative and positive energy [19]. For the computational channels $j > n_p$, with the core state Φ_j at higher energy, the corresponding radial wave functions Θ_j of the $(N+1)$th electron should have fairly negative orbital energies and exponentially decaying radial wave function with negligible magnitude at $r_{N+1} = r_o$. By including sufficient number of computational channels in the ECR calculation, we are able to take into account adequately the electron correlations in our calculation.

Following the details presented earlier [1, 18–21] and similar to the K-matrix in equation (3), the short-range reaction matrix with total angular momentum J is expressed by

$$K_{ij}^J = \sum_\alpha U_{i\alpha} \tan(\pi\nu_\alpha) U_{j\alpha} \tag{6}$$

in terms of the smoothly varying eigenchannel parameters in energy, i.e., eigen-quantum defect ν_α and the $n_p \times n_p$ orthogonal transformation matrix $U_{j\alpha}$. The state functions are then expressed as the linear combination of eigenchannel wavefunctions $\psi_\alpha(E)$, i.e.,

$$\Psi^J(E) = \sum_\alpha A_\alpha \psi_\alpha(E), \tag{7}$$

where A_α is the mixing coefficient and determined by the asymptotic boundary conditions. We shall refer to some of the previous works [1, 10, 11, 19] for detailed computational procedure leading to the calculated spectra.

3. Results and discussions

The ^1P spectra originated from the ground state of Li^+ below the $N = 2$ ionization threshold are already very well characterized in [3] and since the results of our calculation are in good agreement with those earlier results, we do not repeat in this paper the same spectra from the current calculation. Instead, similar to our recent study on the overlapping resonance series for He atom, we will first focus on the spectra from the bound excited $1s2p\ ^1P$ state to all overlapping ^1S and ^1D resonance series, respectively, between the $N = 2$ and $N = 3$ ionization thresholds. In particular, we examine if there is any level crossing between the members of the overlapping resonance series such as the ones for the He atom we discussed recently [1]. Our discussion will continue with the spectra from the ground state and the $1s2s\ ^1S$ bound excited state of the Li^+ ion to all overlapping ^1P resonances series between the $N = 2$ and $N = 3$ thresholds. Comparison with the limited experimental data will be presented. The width of the resonance in the present calculations, as we pointed out earlier, is derived from the energy variation of η_{tot}. We will compare in our subsequent discussion the individual resonance width between our calculation and other earlier calculations [3, 6].

In addition, similar to what we did in [1], by examining in details the state function of each resonance, as it migrates along the resonance series, we are able to check the detailed characteristics of each individual resonance to assure its proper assignment in terms of the probability densities corresponding to the contributing electronic configurations. We will also look into the question if there is strong interaction between closely located neighboring resonances from different resonance series like the ones discussed in [1] and in particularly if there are level crossings between members of the overlapping resonance series and how it is affected by the strong correlation, if any.

3.1. Overlapping ^1D and ^1S autoionizing resonance series

Between the $N = 2$ and $N = 3$ thresholds, theoretically, there are six ^1D autoionization resonance series that decay into four singly ionization ^1D channels (i.e., $1s\epsilon d$, $2s\epsilon d$, $2p\epsilon p$, and $2p\epsilon f$) for the $1s2p\ ^1P \rightarrow\ ^1D$ photoionization. Figure 1 presents the photoionization spectrum for the first few ^1D resonances above the $N = 2$ ionization threshold. It is clear that not only the spectra from the BSK calculation (top plot) and the ECR calculation (bottom plot) are in excellent agreement, the length and velocity results in both calculations are also in good agreement. To facilitate our discussion, we have labeled the six overlapping resonance series as $A_n((2, 0)_n^+)$, $B_n((0, 2)_n^+)$, $C_n((0, 0)_n^+)$, $D_n((1, 1)_n^-)$, $E_n((-2, 0)_n^0)$ and $F_n((-1, 1)_n^0)$ using the classification scheme in the form of $(K, T)_n^A$ discussed earlier [2]. On the energy scale shown in figure 1, the resonance A_4 and D_4 appears to be nearly degenerate. However, as shown in figure 2 with an enlarged energy scale, this pair of resonances are in fact well separated. It is also shown those two resonances are well separated in their respective partial cross sections into the dominating $2s\epsilon d$ and $2p\epsilon p$ ionization channels. A detailed examination of the probability densities from the contributing electronic configurations in our BSK calculation shows that these two resonances do not correlate strongly like the one we have shown

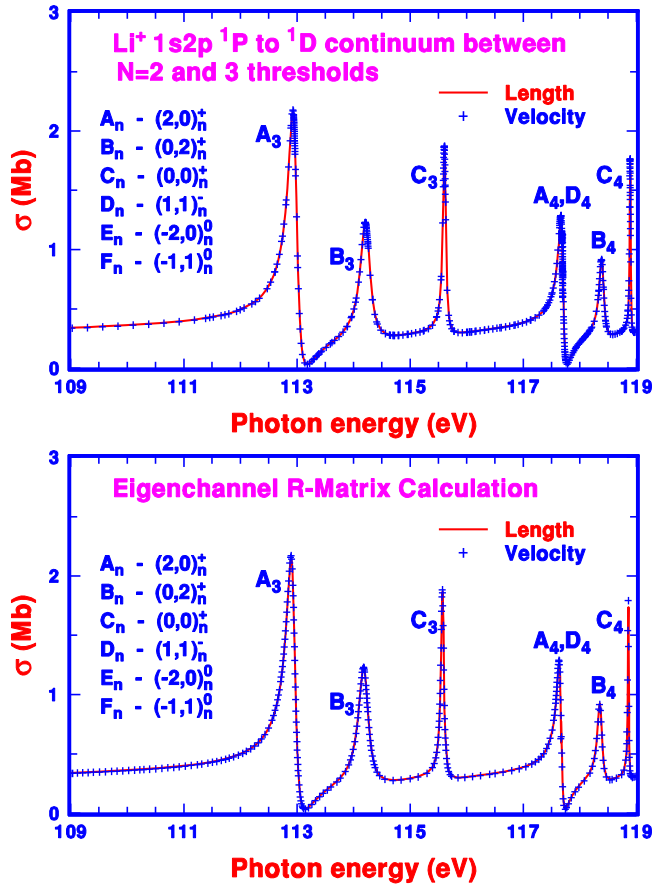

Figure 1. The theoretical photoionization spectra for the first few resonances of Li^+ from the $1s2p\ ^1P$ bound excited state to the ^1D continuum above the $N = 2$ threshold calculated with the BSK method (top plot) and the ECR method (bottom plot). Since the results of the ECR calculation are nearly identical to the ones from the BSK calculation, they will not be shown explicitly in all subsequent figures.

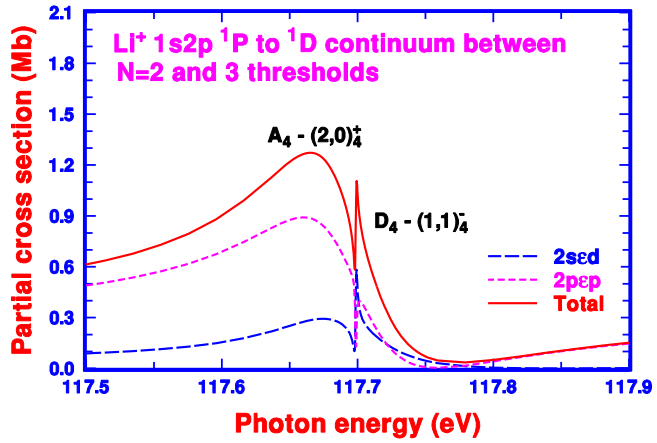

Figure 2. The theoretical photoionization spectra of Li^+ from the $1s2p\ ^1P$ bound excited state to the ^1D continuum for the two neighboring resonances A_4 and D_4 and two of the more dominating partial cross sections into the $2p\epsilon p$ and $2s\epsilon d$ ionization channels.

for He in figures 3 and 4 of [1]. At higher energies shown in figure 3, the resonances D_5 and D_6 are both well separated from their respective neighboring resonances A_5 and A_6. Unlike what we found for He, there is no level crossing such

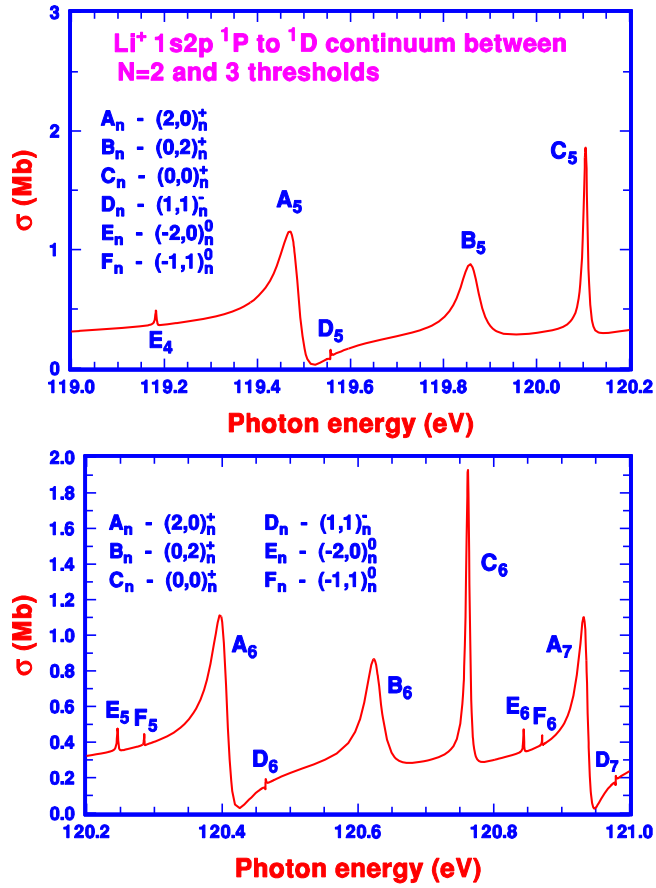

Figure 3. The theoretical photoionization spectra of Li^+ from the $1s2p\ ^1P$ bound excited state to the ^1D continuum between the $N = 2$ and $N = 3$ ionization thresholds from the BSK calculation at higher energies.

as the one shown in figure 3 of [1]. In fact, all six overlapping doubly excited ^1D autoionization series are well separated and the general features of each resonance series appear to be similar as energy increases. Table 1 compares our calculated effective quantum number n^* against the $N = 3$ threshold and the widths of all ^1D resonance series with the ones from the complex-rotation calculation. We should note that with substantial cancellations from large number of contributing terms, the calculated widths are typically accurate to about 4 to 5 digits. As a result, with the widths as small as 10^{-5} Ry, the agreement between these two fairly different calculations is satisfactory.

For the ^1S continua, there are only three resonance series, i.e., $A_n((2, 0)_n^+)$, $B_n((0, 0)_n^+)$, and $C_n((-2, 0)_n^+)$ that decay into three singly ionized channels, $1s\epsilon s$, $2s\epsilon s$, and $2p\epsilon p$. Our calculated spectra are presented in figure 4. It appears that at higher energies, all three resonance series follow their respective similar general features and are all very well separated as shown in the bottom plot of figure 4. On the lower energy side, the pair of resonances C_3 and A_4 are somewhat closely located and in reverse order in energy than their corresponding higher members. A closer look with the enlarged energy scale shown in figure 5, together with the dominating partial cross sections to the $2s\epsilon s$ ionization

Table 1. The calculated Li^+ $^1D^e$ effective quantum numbers n^* and widths Γ (in $a[n] = a \times 10^n$ Ry).

	Present		Reference [6]	
State	n^*	Γ	n^*	Γ
A_3 $^1D^e$	2.419	1.333[−2]	2.418	1.203[−2]
A_4 $^1D^e$	3.449	6.944[−3]	3.445	6.041[−3]
A_5 $^1D^e$	4.419	3.365[−3]	4.414	2.485[−3]
A_6 $^1D^e$	5.402	1.785[−3]	5.395	1.492[−3]
A_7 $^1D^e$	6.390	1.038[−3]	6.384	8.622[−4]
B_3 $^1D^e$	2.600	1.577[−2]	2.598	1.430[−2]
B_4 $^1D^e$	3.748	7.390[−3]	3.740	6.625[−3]
B_5 $^1D^e$	4.755	3.789[−3]	4.748	3.372[−3]
B_6 $^1D^e$	5.755	2.121[−3]	5.748	1.879[−3]
C_3 $^1D^e$	2.859	4.762[−3]	2.850	4.477[−3]
C_4 $^1D^e$	4.014	1.550[−3]	3.997	1.418[−3]
C_5 $^1D^e$	5.016	8.023[−4]	4.998	7.168[−4]
C_6 $^1D^e$	6.009	4.615[−4]	5.991	4.085[−4]
D_4 $^1D^e$	3.451	1.014[−4]	3.450	8.622[−5]
D_5 $^1D^e$	4.479	6.655[−5]	4.479	6.582[−5]
D_6 $^1D^e$	5.490	4.675[−5]	5.490	4.351[−5]
D_7 $^1D^e$	6.496	3.198[−5]	6.496	2.880[−5]
E_4 $^1D^e$	4.199	2.556[−4]	4.192	2.398[−4]
E_5 $^1D^e$	5.186	1.565[−4]	5.182	1.452[−4]
E_6 $^1D^e$	6.179	1.030[−4]	6.174	8.806[−5]
F_5 $^1D^e$	5.237	4.746[−5]	5.224	4.721[−5]
F_6 $^1D^e$	6.239	3.882[−5]	6.221	2.251[−5]

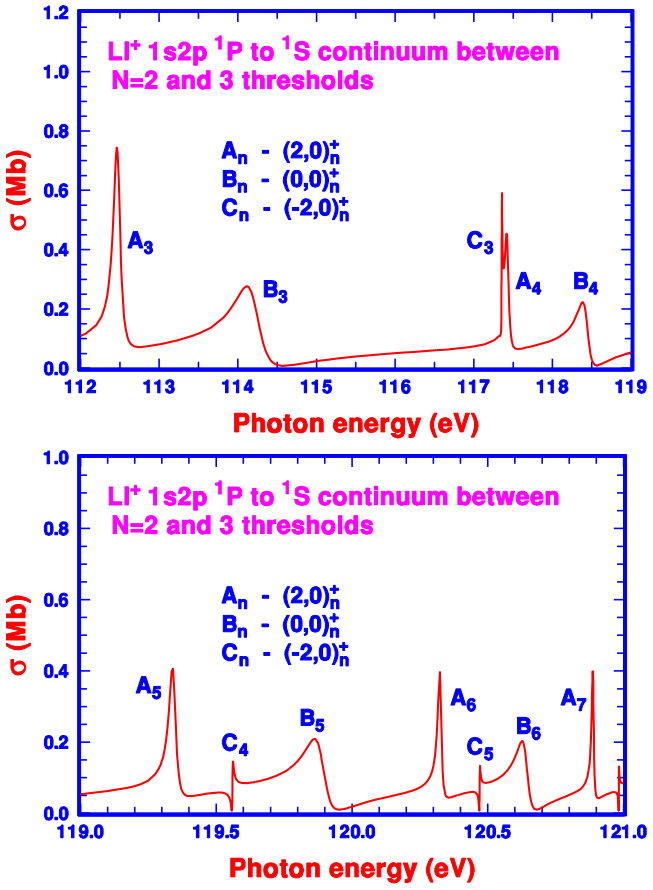

Figure 4. The theoretical photoionization spectra of Li^+ from the $1s2p$ ^1P bound excited state to the ^1S continuum between $N = 2$ and $N = 3$ thresholds from the BSK calculation.

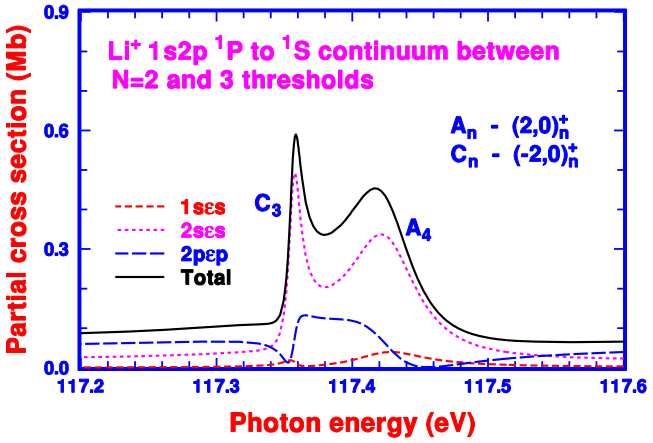

Figure 5. The theoretical photoionization spectra of Li^+ from the $1s2p$ ^1P bound excited state to the ^1S continuum for the two neighboring resonances C_3 and A_4 and their corresponding partial cross sections into all three ionization channels.

channel, indicate that, in spite of the level crossing between these two resonance series, they are actually well separated. A detailed examination of the probability densities from the contributing electronic configurations in our BSK calculation also shows that these two resonances do not correlate strongly like the one we have shown for He in figure 7 of [1]. It is interesting to note that a straightforward extension of the current calculation to Be^{+2} shows that there is no longer the level crossing between the A_n and C_n resonance series such as the ones we have identified for He and Li^+. Finally, table 2 compares our calculated effective quantum number n^* and the widths of all ^1S resonance series with the ones from the complex-rotation calculation. Again, they are in satisfactory agreement for calculated values as small as 10^{-4} Ry shown in table 1 for the ^1D resonance series.

3.2. Overlapping ^1P autoionizing resonance series

For the ^1P continua, there are five autoionization resonance series that decay into four ^1P ionization channels (i.e., $1s\epsilon p$, $2s\epsilon p$, $2p\epsilon s$, and $2p\epsilon d$). Experimentally, due to the limitation of the energy resolution, only the first two members of the ${}_3(1, 1)_n^+$ ^1P resonance series with $n = 3$ and 4 are resolved in the photo-ionized spectra between the $N = 2$ and $N = 3$ thresholds from the ground state of Li^+ ion [3]. The top plot of figure 6 presents our theoretical spectrum of the first five resonances above the $N = 2$ threshold from the Li^+ ground state. Similarly, we have labeled the five overlapping resonance series as $A_n((1, 1)_n^+)$, $B_n((-1, 1)_n^+)$, $C_n((2, 0)_n^-)$, $D_n((0, 0)_n^-)$, and $E_n((-2, 0)_n^o)$. With a peak cross section of a little over 0.42 Mb for A_3 and a value of about 0.4 Mb for A_4, the two dominating resonances from the spectrum shown in figure 6 are in good agreement with the convoluted theoretical

Table 2. The calculated Li^+ $^1S^e$ effective quantum numbers n^* and widths Γ (in $a[n] = a \times 10^n$ Ry).

	Present		Reference [6]	
State	n^*	Γ	n^*	Γ
A_3 $^1S^e$	2.357	7.830[−3]	2.357	7.520[−3]
A_4 $^1S^e$	3.352	4.561[−3]	3.351	4.301[−3]
A_5 $^1S^e$	4.312	2.190[−3]	4.311	2.028[−3]
A_6 $^1S^e$	5.290	1.175[−3]	5.289	1.085[−3]
A_7 $^1S^e$	6.275	6.810[−4]	6.275	6.302[−4]
B_3 $^1S^e$	2.597	2.802[−2]	2.597	2.561[−2]
B_4 $^1S^e$	3.766	1.181[−2]	3.763	1.058[−2]
B_5 $^1S^e$	4.780	6.204[−3]	4.775	5.508[−3]
B_6 $^1S^e$	5.781	3.545[−3]	5.776	3.099[−3]
B_7 $^1S^e$	6.779	2.179[−3]	6.775	1.895[−3]
C_3 $^1S^e$	3.328	7.880[−4]	3.301	9.504[−4]
C_4 $^1S^e$	4.481	3.298[−4]	4.458	3.838[−4]
C_5 $^1S^e$	5.499	1.836[−4]	5.473	2.277[−4]
C_6 $^1S^e$	6.503	1.122[−4]	6.474	1.395[−4]

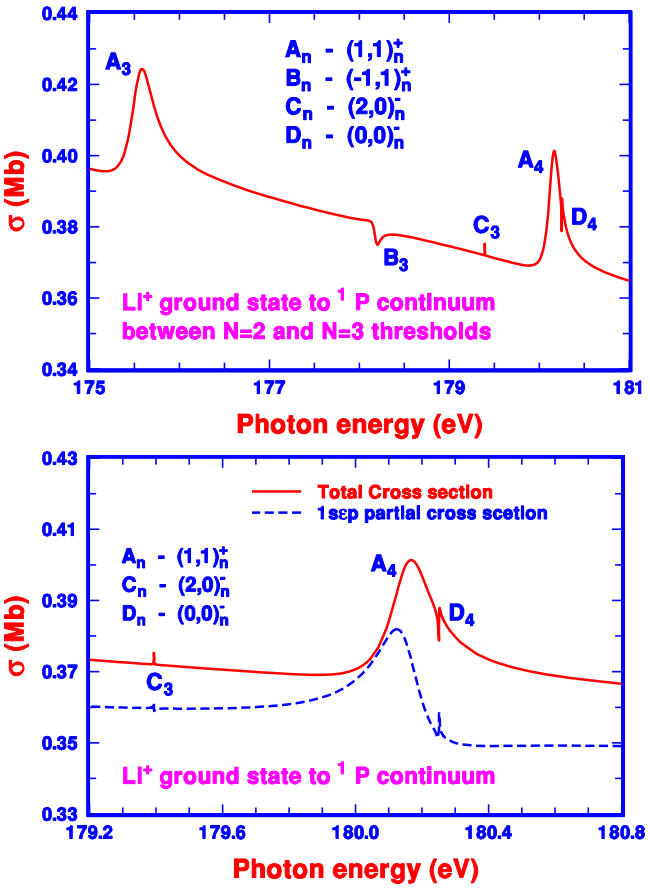

Figure 6. The theoretical photoionization spectrum for the first five resonances of Li^+ from its ground state to the ^1P continuum above the $N = 2$ threshold (top plot) and a more refined theoretical spectrum for the two neighboring resonances A_4 and D_4 together with the dominating partial cross section into the $1s\epsilon p$ ionization channel (bottom plot).

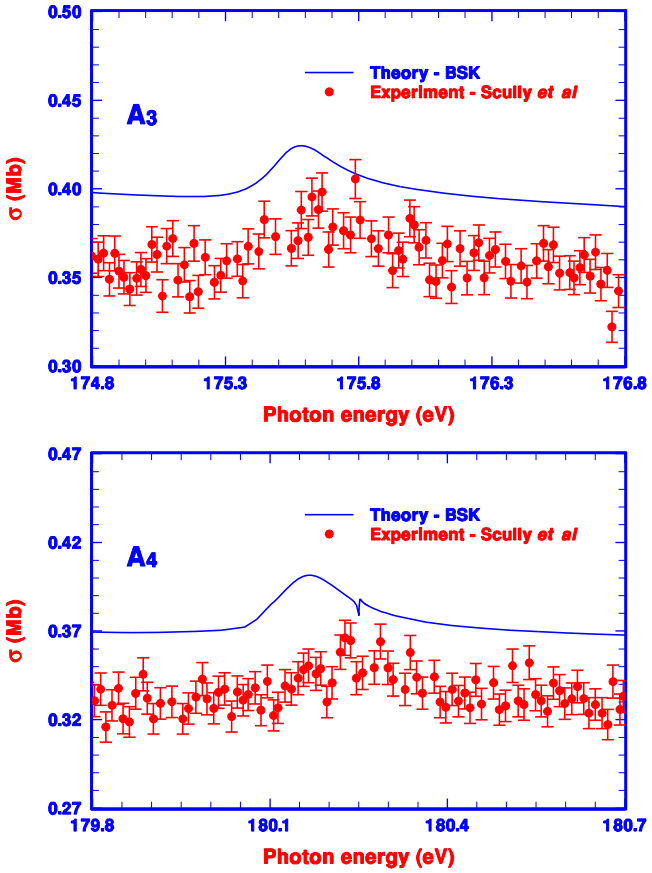

Figure 7. Comparison between the photoionization cross sections near the A_3 and A_4 resonances of ^1P symmetry between the current calculation and the observed spectra from [3].

ones shown in figure 6 of [3]. In addition, we compares our calculated spectra with the observed ones from [3] in figure 7. The slight difference between the peak cross sections of all three theoretical calculations and the observed one may be partly due to the 20% experimental uncertainty and also from the choice of normalizing the observed spectra to the less elaborate theoretical background calculation in the absence of any resonances. Our theoretical spectrum also shows an additional resonance D_4 on the shoulder of the higher energy side of A_4, which was not shown in the convoluted spectrum, nor in the experimental spectrum in [3]. A more detailed spectrum with enlarged energy scale from the bottom plot of figure 6 shows that the pair of resonances A_4 and D_4 are well separated and are both dominated by their respective partial cross section into the $1s\epsilon p$ ionization channel. As the resonance series migrate to higher energies, similar to what we have shown for the ^1S and ^1D continua, all five resonance series follow their respective similar general features and are all very well separated as shown in figure 8. We do not find strong correlation between members from different resonance series either.

Figure 9 presents our calculated photo-ionized spectra from the metastable $1s2s$ ^1S state of Li^+. The resonance series B_n, with more substantial overlap between the initial and final continua, becomes as dominant as the broader A_n series. Again, as expected, all resonance series follow their respective general

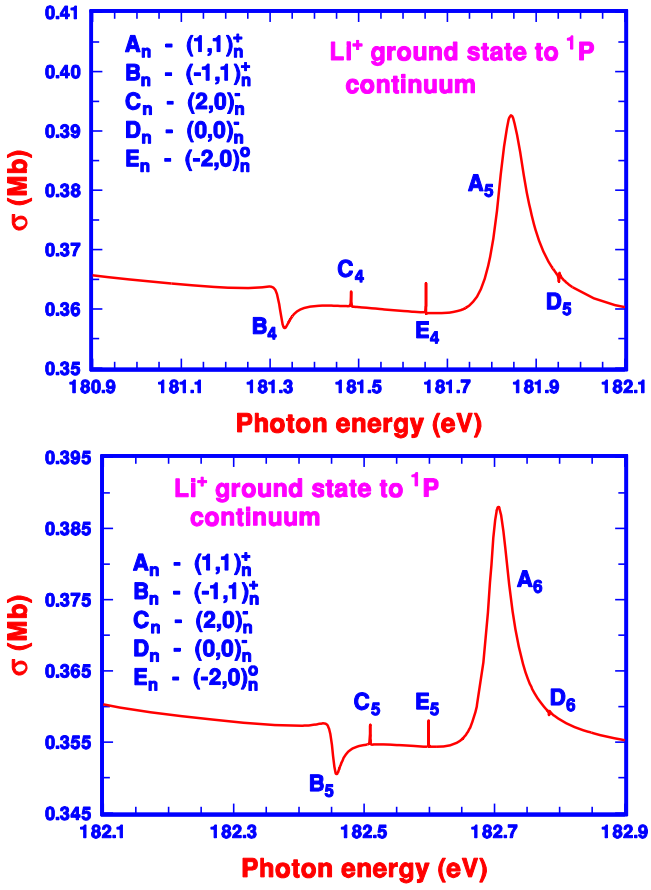

Figure 8. The theoretical photoionization spectra of Li^+ from its ground state to the ^1P continuum between the $N = 2$ and $N = 3$ ionization thresholds from the BSK calculation at higher energies.

features at higher energies and are all very well separated. The closely located resonances A_4 and D_4 are similarly well separated as shown in figure 10, but, unlike the ^1P photoionization from the ground state, the partial cross sections are now dominated by the ionization into $2s\epsilon p$ and $2p\epsilon d$ continua. Similar to what we found for the ^1S and ^1D resonance series, our calculated effective quantum number n^* and the widths for all five ^1P resonance series are in satisfactory agreement with the ones from the complex-rotation calculation shown in table 3. The slight difference in the calculated widths of resonances A_3 and A_4 between our calculation and that from [3, 6] may be attributed to the contributions from the multiple continua which are included explicitly in the present calculation whereas such contributions are indirectly represented in the earlier calculations by optimized local orbitals.

4. Conclusions

With essentially identical results between the BSK and ECR calculations, we present in this paper a reliable theoretical estimate of the photoionization spectra from the ground and the bound excited $1s2s\ ^1S$ and $1s2p\ ^1P$ states of Li^+ to the continua with multiple ionization channels between the $N = 2$ and $N = 3$ ionization thresholds. Unlike the charge-neutral He atom, which we studied in detail earlier [1], the

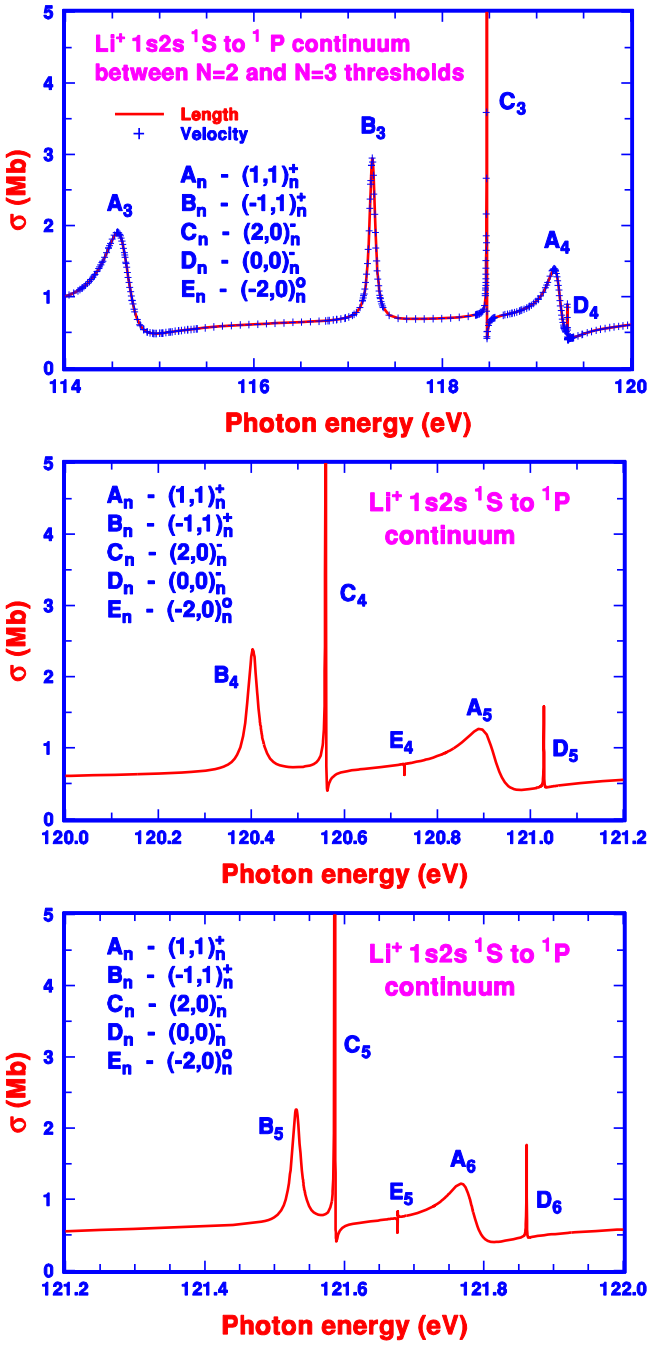

Figure 9. The theoretical photoionization spectra of Li^+ from its metastable $1s2s\ ^1S$ state to the ^1P continuum between the $N = 2$ and $N = 3$ ionization thresholds from the BSK calculation.

degenerate ionization thresholds of the heavier two-electron atomic systems do not lead to strong correlations between neighboring resonances and, in turn, could not be linked directly to the only level crossing between the C_3 and $A_4\ ^1S$ resonances identified between resonance series for Li^+, nor the lack of such level crossing for Be^{2+} in the present study. However, a detailed examination of the state functions of individual doubly excited resonance shows that all resonances are still characterized by a large number of two-electron orbits corresponding to electron configurations with multiple $\ell_1\ell_2$ combinations. This is very different from the doubly excited

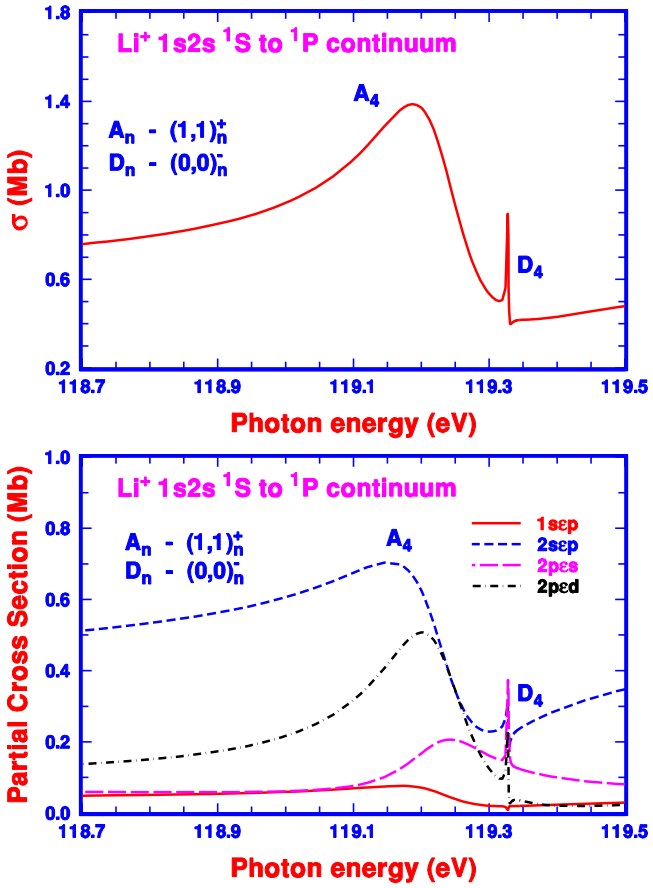

Figure 10. The theoretical photoionization spectra (top plot) of Li^+ from its metastable $1s2s\ ^1S$ state to the ^1P continuum for the two neighboring resonances, A_4 and D_4, and the corresponding partial cross sections into all four ionization channels (bottom plot).

resonances from atomic systems which do not have degenerate ionization threshold where the doubly excited resonances are generally characterized by the *LS* coupling corresponding to dominating electronic configurations with a single $\ell_1\ell_2$ combination. As a result, even with a fairly weak interaction between neighboring resonances, it remains essential that all resonance series for all two-electron ions be classified in terms of the set of correlated quantum numbers (K, T, and A) in the form of $(K, T)^A_n$, such as the one for the He atom due to the degenerate ionization thresholds. With all the resonances clearly identified, our study offers an interesting challenge for further experimental observation with higher energy resolution.

Acknowledgments

This work was supported by the MOST in Taiwan under Grant No. MOST 104-2112-M-030-001, the National Natural Science Foundation of China under Grant Nos. U1530401 and 11274035, the Special Program for Applied Research on Super Computation of the NSFC-Guangdong Joint Fund, the National High-Tech ICF Committee in China and Open Research Fund Program of the State Key Laboratory of Low-Dimensional Quantum Physics, Tsinghua University. We also acknowledge the computational support from the Beijing Computational Science Research Center (CSRC). In addition, TNC is thankful for the partial support from NCTS in Taiwan.

Table 3. The calculated $Li^+\ ^1P^o$ effective quantum numbers n^* and widths Γ (in $a[n] = a \times 10^n$ Ry).

	Present		Reference [6]	
State	n^*	Γ	n^*	Γ
$A_3\ ^1P^o$	2.466	2.187[−2]	2.467	2.079[−2]
$A_4\ ^1P^o$	3.554	1.131[−2]	3.543	1.056[−2]
$A_5\ ^1P^o$	4.533	5.620[−3]	4.530	5.254[−3]
$A_6\ ^1P^o$	5.524	3.055[−3]	5.522	2.845[−3]
$B_3\ ^1P^o$	2.938	5.363[−3]	2.932	4.968[−3]
$B_4\ ^1P^o$	4.150	1.905[−3]	4.142	1.755[−3]
$B_5\ ^1P^o$	5.175	1.114[−3]	5.165	1.012[−3]
$B_6\ ^1P^o$	6.180	6.952[−4]	6.170	6.312[−4]
$C_3\ ^1P^o$	3.269	9.135[−5]	3.269	9.026[−5]
$C_4\ ^1P^o$	4.257	6.692[−5]	4.257	6.619[−5]
$C_5\ ^1P^o$	5.248	4.298[−5]	5.248	4.252[−5]
$C_6\ ^1P^o$	6.241	2.807[−5]	6.241	2.745[−5]
$D_4\ ^1P^o$	3.585	1.578[−4]	3.584	1.391[−4]
$D_5\ ^1P^o$	4.634	7.564[−5]	4.634	6.732[−5]
$D_6\ ^1P^o$	5.655	4.602[−5]	5.655	4.005[−5]
$D_7\ ^1P^o$	6.666	2.959[−5]	6.666	2.568[−5]
$E_4\ ^1P^o$	4.382	1.820[−5]	4.373	1.309[−5]
$E_5\ ^1P^o$	5.371	1.078[−5]	5.358	7.615[−6]

References

[1] Chang T N, Fang T K and Gao X 2015 *Phys. Rev.* A **91** 023403
[2] Lin C D 1983 *Phys. Rev. Lett.* **51** 1348
Sinanoğlu O and Herrick D R 1975 *J. Chem. Phys.* **62** 886
[3] Scully S W J *et al* 2006 *J. Phys. B: At. Mol. Opt. Phys.* **39** 3957
[4] Mosnier J P, Costello J, Kennedy E and Whitty W 2000 *J. Phys. B: At. Mol. Opt. Phys.* **33** 5203
[5] Kiernan L M, Kennedy E T, Mosnier J P, Costello J T and Sonntag B F 1994 *Phys. Rev. Lett.* **72** 2359
Diehl S, Cubaynes D, Bizau J M, Wuilleumier F J, Kennedy E T, Mosnier J P and Morgan T J 1999 *J. Phys. B: At. Mol. Opt. Phys.* **32** 4193
[6] Chung K T and Lin C D 1998 *At. Data Nucl. Data Tables* **69** 101
[7] Berrington K A and Nakazaki S 1998 *J. Phys. B: At. Mol. Opt. Phys.* **31** 313
[8] Chang T N 1993 *Many-Body Theory of Atomic Structure and Photoionization* ed T N Chang (Singapore: World Scientific) pp 213–47
[9] Fang T K and Chang T N 2000 *Phys. Rev.* A **61** 062704
[10] Gao X and Li J-M 2012 *Chin. Phys. Lett.* **29** 033101
[11] Gao X and Li J-M 2014 *Phys. Rev.* A **89** 022710
[12] Starace A F 1982 *Handbuch der Physik, Theory of Atomic Photoionization* ed W Mehlhorn (Berlin: Springer) pp 1–121

[13] Carravetta V, Spizzo P and Moccia R 1993 *Many-Body Theory of Atomic Structure and Photoionization* ed T N Chang (Singapore: World Scientific) pp 175–212
[14] Aiba K, Igarashi A and Shimamura I 2007 *J. Phys. B: At. Mol. Opt. Phys.* **40** F9
[15] Burke P G 2011 *R-Matrix Theory of Atomic Collisions: Application to Atomic, Molecular and Optical Processes* (Berlin: Springer)
[16] Burke P G and Robb W D 1975 *Adv. At. Mol. Phys.* **11** 143
Berrington K A, Eissner W B and Norrington P H 1995 *Comput. Phys. Commun.* **92** 290
Seaton M J 1985 *J. Phys. B: At. Mol. Phys.* **18** 2111
Berrington K A, Burke P G, Butler K, Seaton M J, Storey P J, Taylor K T and Yan Y 1987 *J. Phys. B: At. Mol. Phys.* **20** 6379
[17] Chang J J 1977 *J. Phys. B: At. Mol. Phys.* **10** 3335
Norrington P H and Grant I P 1987 *J. Phys. B: At. Mol. Phys.* **20** 4869
Ait-Tahar S, Grant I P and Norrington P H 1996 *Phys. Rev.* A **54** 3984
[18] Li J M, Ky L V, Qu Y Z, Yan J, Zhang P H, Zhou H L and Faucher P 1997 *Phys. Rev.* A **55** 3239
Han X Y and Li J M 2006 *Phys. Rev.* A **74** 062711
[19] Aymar M, Greene C H and Lue-Koenig E 1996 *Rev. Mod. Phys.* **68** 1015
[20] Fano U and Lee J M 1973 *Phys. Rev. Lett.* **31** 1573
Lee C M 1974 *Phys. Rev.* A **10** 584
[21] Huang W, Zou Y, Tong X M and Li J M 1995 *Phys. Rev.* A **52** 2770
Lee C M and Lu K T 1973 *Phys. Rev.* A **8** 1241
[22] Seaton M J 1983 *Rep. Prog. Phys.* **46** 167